

Dynamic Modeling of Sparse Longitudinal Data and Functional Snippets With Stochastic Differential Equations

Yidong Zhou and Hans-Georg Müller*

Department of Statistics, University of California, Davis
Davis, CA 95616, USA

April 2023

Abstract

Sparse functional/longitudinal data have attracted widespread interest due to the prevalence of such data in social and life sciences. A prominent scenario where such data are routinely encountered are accelerated longitudinal studies, where subjects are enrolled in the study at a random time and are only tracked for a short amount of time relative to the domain of interest. The statistical analysis of such functional snippets is challenging since information for the far-off-diagonal regions of the covariance structure is missing. Our main methodological contribution is to address this challenge by bypassing covariance estimation and instead modeling the underlying process as the solution of a data-adaptive stochastic differential equation. Taking advantage of the interface between Gaussian functional data and stochastic differential equations makes it possible to efficiently reconstruct the target process by estimating its dynamic distribution. The proposed approach allows one to consistently recover forward sample paths from functional snippets at the subject level. We establish the existence and uniqueness of the solution to the proposed data-driven stochastic differential equation and derive rates of convergence for the corresponding estimators. The finite-sample performance is demonstrated with simulation studies and functional snippets arising from a growth study and spinal bone mineral density data.

Keywords: accelerated longitudinal study, dynamic distribution, empirical dynamic, growth monitoring, sparse functional data.

*Yidong Zhou is Graduate Student Researcher and Hans-Georg Müller is Professor at the Department of Statistics, University of California, Davis. This work was partially supported by NSF (DMS-20146260) and NIH (ECHO).

1 Introduction

Functional data are commonly viewed as i.i.d. samples of realizations of an underlying smooth stochastic process, which is typically observed at a discrete grid of time points. Such data are common and routinely arise in longitudinal studies. Functional data analysis has received much attention over the last decades, and functional principal component analysis (Kleffe 1973; Castro et al. 1986; Hall and Hosseini-Nasab 2006; Chen and Lei 2015; Zhou et al. 2022) and functional regression (Ramsay and Silverman 2005; Yao et al. 2005b; Hall and Horowitz 2007) have emerged as key tools. Detailed introductions and reviews can be found in Ramsay and Silverman (2005); Hsing and Eubank (2015); Wang et al. (2016). One area where there are still important open questions concerns the impact of the study design on the analysis. We develop here a novel type of analysis for functional snippets, which correspond to very sparse sampling designs that arise often in accelerated longitudinal studies, by establishing a connection to stochastic differential equations (SDE).

From a general perspective, functional data are collected through various study designs, where one can differentiate between fully observed, densely and sparsely sampled functional data (Zhang and Wang 2016). Fully observed functional data occur in continuous sensor signal recordings and dense designs when measurements at a large number of well-spaced time points are available. Sparse designs are characterized by the availability of only a small number of measurements. A common sparse design occurs when sparse time points are distributed over the entire domain for each subject, with a smooth density that is strictly positive over the time domain where data are collected (Yao et al. 2005a; Hall et al. 2006; Li and Hsing 2010).

In this paper, the focus is on a second type of sparse design that occurs in accelerated longitudinal studies (Galbraith et al. 2017), where subjects are enrolled in the study at a random time within the time domain and are only tracked for a limited amount of time

relative to the domain of interest. Such accelerated longitudinal designs are appealing for practitioners in social and life sciences as they minimize the time and resources required to collect data for each subject, especially when data gathering is costly, intrusive or difficult. Formally, denoting the domain of interest by $\mathcal{T} = [a, b]$, the i th subject is only observed on a sub-interval $[A_i, B_i] \subset \mathcal{T}$ where $B_i - A_i \leq \eta(b - a)$ for all i and $\eta \in (0, 1)$ is a constant. Such data, when the constant η is much smaller than 1, are referred to as functional snippets (Lin et al. 2021).

Partially observed functional data also arise in the form of functional fragments (Descary and Panaretos 2019; Liebl and Rameseder 2019; Kneip et al. 2020), where the constant δ can be nearly as large as 1. The presence of large fragments makes such functional fragments easier to handle since the design plot (Yao et al. 2005a) is typically fully or nearly fully covered by the design points, thereby enabling the estimation of the covariance surface directly from the data. In contrast, all of the design points for functional snippets fall within a narrow band around the diagonal area, where the domain of interest is much larger than this band. It is therefore not possible to infer the covariance surface of the functional data with the usual nonparametric approach and this impedes the implementation of functional principal component analysis and all related methods. The only known solution is to impose additional and typically very strong and often unverifiable assumptions about the nature of the covariance. Such assumptions have been made to justify various forms of covariance completion that have included parametric, semiparametric and other approaches.

For the modeling of time-dynamic systems, empirical dynamics for functional data (Müller and Yao 2010) is an approach to recover the underlying dynamics from repeated observations of the trajectories that are generated by the dynamics, including a nonlinear version (Verzelen et al. 2012). These approaches do not cover functional snippets. To the best of our knowledge, Dawson and Müller (2018) is the only existing dynamic approach aimed at the analysis of functional snippets, where the underlying dynamics are investigated

through an autonomous differential equation for longitudinal quantile trajectories, requiring the underlying process to be monotonic (Abramson and Müller 1994; Vittinghoff et al. 1994) and is aimed at estimating the conditional quantile trajectories given an initial condition, rather than the whole dynamic distribution.

Here we aim to reconstruct the latent stochastic process that generates the observed functional snippet data by recovering its dynamic distribution. To overcome the challenge posed by snippets, we model the underlying process as the solution of a data-adaptive SDE. The dynamic distribution of the target process, containing all information about the underlying dynamics, is then estimated by stepwise forward integration. SDEs have been used previously for the modeling of functional data (Comte and Genon-Catalot 2020; Denis et al. 2021) with a focus on the estimation of drift and/or diffusion coefficients with parametric components and in the setting of fully observed functional data. In contrast, the SDE approach we propose here is nonparametric and does not include parametric components.

The proposed SDE approach is novel and in contrast to the various covariance completion approaches it is nonparametric and does not involve functional principal component analysis. The latter requires to recover the complete covariance surface, which is straightforward for dense designs (He et al. 2000), but for functional snippets in principle is impossible, unless one is prepared to impose strong assumptions about the global structure of the covariance that cannot be verified. The utility of the proposed approach for statistical practice is illustrated for growth and bone mineral density data in Section 6, where it is shown to aid in growth monitoring and more generally distinguishing individuals with abnormal development patterns. The proposed approach can make predictions for individuals with only one observation, where the individual-specific dynamic distribution far into the future can be obtained. The rate of convergence for the corresponding conditional distributions is derived in terms of the Wasserstein metric. The main assumption of the

proposed approach is that the underlying process is Gaussian.

The specific contributions of this paper are, first, to provide an alternative perspective to characterize functional snippets using SDEs; second, to recover future distributions of individual subjects under minimal assumptions; third, to provide an approach that works for minimal snippets, where only two adjacent measurements may be available for each subject; fourth, to demonstrate existence and uniqueness of the solution to the data-adaptive SDE, along with the rate of convergence for the corresponding estimate; fifth, we demonstrate the wide applicability of the proposed dynamic modeling approach with growth snippets from Nepalese children and also with bone mineral density data.

The rest of this paper is organized as follows. In Section 2 we introduce the proposed dynamic model, while Section 3 covers estimation procedures. Theoretical results are established in Section 4. Simulations and applications for a Nepalese growth study data and spinal bone mineral density data are discussed in Sections 5 and 6, respectively. Finally, we conclude with a brief discussion in Section 7.

2 Learning Dynamic Distribution via Stochastic Differential Equations

2.1 Stochastic differential equations and diffusion processes

A typical (Itô) stochastic differential equation (SDE) takes the form

$$\begin{cases} dX_t = b(t, X_t)dt + \sigma(t, X_t)dB_t, & t \in \mathcal{T}, \\ X_0 = x_0, \end{cases} \quad (1)$$

where $X_t = X(t)$ is a stochastic process on (Ω, \mathcal{F}, P) , b and σ are the drift and diffusion coefficients, respectively, and B_t is a Brownian motion (also known as Wiener process).

The initial value x_0 can be either deterministic or random, independent of the Brownian motion B_t . It is known that a unique solution of (1) exists if the Lipschitz condition

$$|b(t, x) - b(t, y)| + |\sigma(t, x) - \sigma(t, y)| \leq C|x - y| \quad \text{for all } x, y \in \mathbb{R}, t \in \mathcal{T}. \quad (2)$$

and the linear growth condition

$$|b(t, x)| + |\sigma(t, x)| \leq C(1 + |x|) \quad \text{for all } x \in \mathbb{R}, t \in \mathcal{T}, \quad (3)$$

hold for some constant $C > 0$ (Oksendal 2013, chap. 5.2). In fact, if coefficients b and σ satisfy the Lipschitz and linear growth conditions, then any solution X_t is a diffusion process on \mathcal{T} with drift coefficient b and diffusion coefficient σ (Panik 2017, p. 154). A diffusion process is a continuous-time Markov process that has continuous sample paths, which can be defined by specifying its first two moments together with the requirement that there are no instantaneous jumps over time. By definition, we can write the formulae for the drift and diffusion coefficients of a diffusion process in the following form:

$$b(t, x) = \lim_{s \rightarrow t^+} \frac{1}{s - t} E(X_s - X_t | X_t = x) \quad (4)$$

and

$$\sigma^2(t, x) = \lim_{s \rightarrow t^+} \frac{1}{s - t} E\{(X_s - X_t)^2 | X_t = x\}.$$

Note that the diffusion coefficient can be equivalently defined as

$$\sigma^2(t, x) = \lim_{s \rightarrow t^+} \frac{1}{s - t} \text{Var}(X_s - X_t | X_t = x) \quad (5)$$

since

$$\begin{aligned} \text{Var}(X_s - X_t | X_t = x) &= E\{(X_s - X_t)^2 | X_t = x\} - \{b(t, x)(s - t) + o(s - t)\}^2 \\ &= E\{(X_s - X_t)^2 | X_t = x\} + o(s - t). \end{aligned}$$

Here, $b(t, X_t)$ may be thought of as the instantaneous rate of change in the mean of the process given X_t ; and $\sigma^2(t, X_t)$ can be viewed as the instantaneous rate of change of the squared fluctuations of the process given X_t (Kloeden and Platen 1999, chap. 1.7).

Diffusion processes originate in physics as mathematical models of the motions of individual molecules undergoing random collisions with other molecules (Pavliotis 2014). Brownian motion is the simplest and most pervasive diffusion process. Several more complex processes can be constructed from standard Brownian motion, including the Brownian bridge, geometric Brownian motion and the Ornstein-Uhlenbeck process (Uhlenbeck and Ornstein 1930). When drift and diffusion components of a diffusion process are moderately smooth functions, its transition density satisfies partial differential equations, i.e., the Kolmogorov forward (Fokker-Planck) and the Kolmogorov backward equation.

2.2 Alternative formulation of stochastic differential equations

We assume that the observed snippets are generated by an underlying stochastic process X_t defined on some compact domain $\mathcal{T} \subset \mathbb{R}$ with mean function $\mu(t) = E(X_t)$, and covariance function $\Sigma(s, t) = \text{Cov}(X_s, X_t)$. Without loss of generality, \mathcal{T} is taken to be $[0, 1]$ in the sequel. Suppose $\{X_{t,1}, \dots, X_{t,n}\}$ is an independent random sample of X_t , where n is the sample size. In practice, each $X_{t,i}$ is only recorded at subject-specific N_i time points T_{i1}, \dots, T_{iN_i} and the observed data are $Y_{ij} = X_{T_{ij},i}$ for $j = 1, \dots, N_i$. We assume that $N_i > 1$ for the subjects used to learn the SDE as subjects with only one measurement do not carry information about the local covariance structure. The snippet nature is reflected by the restriction that $|T_{ij} - T_{ik}| \leq \delta$ for all i, j, k , and some constant $\delta \in (0, 1)$. The focus of this paper is to infer stochastic dynamics of the underlying stochastic process X_t from data pairs (T_{ij}, Y_{ij}) , $i = 1, \dots, n$, $j = 1, \dots, N_i$. Specifically, we are interested in estimating sample paths of X_t starting from some initial time point given a starting value. The proposed approach borrows information from subjects with at least two measurements in order to recover the subject-specific dynamic distribution far into the future for each participant, even for those with a single measurement, which do not contribute to the model fitting step. For ease of presentation, we assume $N_i = 2$ for all i . Discussion on how to

handle situations where $N_i > 2$ can be found in Section 6.1.

The underlying stochastic process X_t is assumed to follow a general SDE as per (1). In real data applications, the drift and diffusion coefficients in (1) are typically unknown. To recover the underlying dynamics of X_t , instead of attempting to directly estimate the drift and diffusion terms, which is challenging for functional snippet data, we plug in representations (4) and (5) of drift and diffusion coefficients to obtain the following alternative version of the SDE,

$$\begin{cases} dX_t = \left. \frac{\partial}{\partial s} E(X_s|X_t) \right|_{s=t} \cdot dt + \left\{ \left. \frac{\partial}{\partial s} \text{Var}(X_s|X_t) \right|_{s=t} \right\}^{1/2} \cdot dB_t, & t \in \mathcal{T}, \\ X_0 = x_0. \end{cases} \quad (6)$$

Note that s is taken to be strictly greater than t when calculating the partial derivatives of $E(X_s|X_t)$ and $\text{Var}(X_s|X_t)$ with respect to s , in which case the diffusion coefficient is well-defined and not equal to 0. SDE (6) is the key tool to obtain sample paths of X_t given an initial condition by means of a recursive procedure, where under Gaussian assumption at each step the distribution of X_t is constructed using the estimation of conditional means $E(X_s|X_t)$ and conditional variances $\text{Var}(X_s|X_t)$.

Examples of the SDE as per (6) include Brownian motion, Ho-Lee model (Ho and Lee 1986), and Ornstein-Uhlenbeck process (Uhlenbeck and Ornstein 1930), among others. Different models postulate different forms of b and σ . The Brownian motion B_t , with extensive applications in physics and electronics engineering, is a special case of this SDE with zero drift and unit diffusion. The Ho-Lee model $dX_t = g(t)dt + \sigma dB_t$ with $\sigma > 0$ and g a deterministic function of time is a stochastic interest rate model widely used, for instance, for the pricing of bond options and to model future interest rates. The Ornstein-Uhlenbeck process $dX_t = -\theta X_t dt + \sigma dB_t$ with $\theta > 0, \sigma > 0$ is often used to describe mean-reverting phenomena in the physical sciences, evolutionary biology and finance. The coefficient θ characterizes the restoring force towards the mean and σ characterizes the

degree of volatility around the mean value.

3 Estimation

3.1 Simulating sample paths

To estimate sample paths of X_t given an initial condition from function snippets, it is instructive to rewrite the SDE in (6) as

$$\begin{aligned} & \lim_{s \rightarrow t^+} (X_s - X_t) \\ &= \lim_{s \rightarrow t^+} \left\{ \frac{E(X_s|X_t) - E(X_t|X_t)}{s - t} (s - t) + \left\{ \frac{\text{Var}(X_s|X_t) - \text{Var}(X_t|X_t)}{s - t} \right\}^{1/2} (B_s - B_t) \right\} \end{aligned}$$

with an initial condition $X_0 = x_0$. The above formula gives rise to a method to simulate the continuous-time process X_t at a set of discrete time points given an initial condition. Consider the time grid $0 \leq t_0 < t_1 < \dots < t_{K-1} < t_K \leq 1$ and, without loss of generality, assume the time spacing $t_k - t_{k-1}$ is the same for $k = 1, \dots, K$. Denote the common time spacing by Δ , the initial value of X_t at t_0 by X_0 and the simulation of X_t at t_k by X_k for $k = 1, \dots, K$. We then simulate the continuous-time process X_t at the discrete time points $t_k, k = 1, \dots, K$, given an initial condition $X_0 = x_0$, by the recursion

$$\begin{aligned} & X_k - X_{k-1} \\ &= \frac{E(X_k|X_{k-1}) - E(X_{k-1}|X_{k-1})}{\Delta} \Delta + \left\{ \frac{\text{Var}(X_k|X_{k-1}) - \text{Var}(X_{k-1}|X_{k-1})}{\Delta} \right\}^{1/2} (B_{t_k} - B_{t_{k-1}}). \end{aligned}$$

Observing that $E(X_{k-1}|X_{k-1}) = X_{k-1}$, $\text{Var}(X_{k-1}|X_{k-1}) = 0$, and $(B_{t_k} - B_{t_{k-1}})/\sqrt{\Delta} \sim N(0, 1)$, the above recursion reduces to

$$X_k = E(X_k|X_{k-1}) + \{\text{Var}(X_k|X_{k-1})\}^{1/2} W_k, \quad X_0 = x_0, \quad (7)$$

where $W_k \sim N(0, 1)$ are independent for $k = 1, \dots, K$.

We emphasize that under Gaussian assumption on the process X_t , the recursion in (7) generates an exact simulation (Glasserman 2004) of X_t at t_1, \dots, t_K in the sense that the X_k it produces follows the same distribution of the process X_t at t_k for all $k = 1, \dots, K$; see Lemma 1 in Section 4. Classical simulation methods for SDEs, such as the Euler-Maruyama method and the Milstein method (Kloeden and Platen 1999), in general, introduce discretization error at t_1, \dots, t_K , because the increments do not have exactly the right mean and variance. To simulate X_t using recursion (7), there is hence no need to consider increasing numbers of discrete time points K . In practice and particularly for the case of accelerated longitudinal studies, a good rule of thumb is to set the time spacing Δ as the scheduled (as opposed to actual) visit spacing for each subject. The number of discrete time points K to simulate X_t is then determined by the time spacing Δ and the time interval of interest; see Section 6 for the selection of time grids in real data applications.

To estimate sample paths of the process X_t , one needs to iteratively generate a random sample from $N\{E(X_k|X_{k-1}), \text{Var}(X_k|X_{k-1})\}$ to simulate X_t at t_k for $k = 1, \dots, K$. In practice, both the conditional mean $E(X_k|X_{k-1})$ and conditional variance $\text{Var}(X_k|X_{k-1})$ are unknown. One thus has to obtain their estimates to proceed.

3.2 Estimation of conditional mean and conditional variance

Note that the information contained in $X_{k-1} = X_{t_{k-1}}$ is twofold and consists of X_{k-1} itself and also of the time index t_{k-1} . One can then formulate the estimation of the conditional mean $E(X_k|X_{k-1})$ and conditional variance $\text{Var}(X_k|X_{k-1})$ as a regression problem with the response being X_k and the predictor being $(X_{k-1}, t_{k-1})^\top$. For this stepwise prediction approach the training data set consists of the observed snippet data, and the training of the model is described in the following.

Recall the assumption that each subject is observed at two time points T_{i1} and T_{i2} , with measurements denoted by Y_{i1} and Y_{i2} . Let $Z_i = (Y_{i1}, T_{i1})^\top$ and with a slight abuse of

notation set $Y_i = Y_{i2}$ for $i = 1, \dots, n$. Viewing the $\{(Z_i, Y_i)\}_{i=1}^n$ as i.i.d. realizations of the pair of random variables (Z, Y) , consider the regression model

$$Y_i = m(Z_i) + v(Z_i)\epsilon_i, \quad (8)$$

where $m(z) = E(Y|Z = z)$ and $v^2(z) = \text{Var}(Y|Z = z)$ are respectively the conditional mean function and conditional variance function. The error term ϵ_i satisfies $E(\epsilon_i|Z_i) = 0$ and $\text{Var}(\epsilon_i|Z_i) = 1$. Note that the predictor Z_i in this model is two-dimensional so that nonparametric estimation of the conditional mean $E(X_k|X_{k-1})$ and conditional variance $\text{Var}(X_k|X_{k-1})$ by smoothing methods such as local linear regression (Müller 1987; Fan and Gijbels 1996) is feasible.

Both the estimation of conditional means and of conditional variances with parametric or nonparametric regression approaches have been well investigated. For the estimation of conditional variance we adopt the well-known approach of fitting a regression model for the squared residuals $\{Y_i - \hat{m}(Z_i)\}^2$ as responses and Z_i as predictors (Fan and Yao 1998); see Section S.2 of the Supplementary Material for more details. With estimates of the conditional mean function $\hat{m}(\cdot)$ and the conditional variance function $\hat{v}^2(\cdot)$ in hand, conditional means $E(X_k|X_{k-1})$ and conditional variances $\text{Var}(X_k|X_{k-1})$ in (7) are easily obtained by evaluating $\hat{m}(\cdot)$ and $\hat{v}^2(\cdot)$ at $\hat{Z}_{k-1} = (\hat{X}_{k-1}, t_{k-1})^\top$. The corresponding recursive procedure to obtain X_t at t_1, \dots, t_K is

$$\begin{aligned} \hat{X}_1 &= \hat{m}(Z_0) + \hat{v}(Z_0)W_1, \\ \hat{X}_k &= \hat{m}(\hat{Z}_{k-1}) + \hat{v}(\hat{Z}_{k-1})W_k, \quad k = 2, \dots, K, \end{aligned} \quad (9)$$

where $Z_0 = (x_0, t_0)^\top$ and $\hat{Z}_{k-1} = (\hat{X}_{k-1}, t_{k-1})^\top$ for $k = 2, \dots, K$. Algorithm 1 describes how to obtain estimated sample paths for the process X_t .

If one has no prior knowledge about the conditional mean and conditional variance structure, which is often the case in real data applications, one will naturally adopt nonparametric approaches that are more flexible than say multiple linear regression, while

Algorithm 1: Estimating sample paths

Input: training data $\{(Z_i, Y_i)\}_{i=1}^n$, initial condition $Z_0 = (x_0, t_0)^\top$, and time discretization $\{t_k, k = 0, \dots, K\}$.

Output: $(\hat{X}_0, \dots, \hat{X}_K)^\top$.

```
1 for  $k = 1, \dots, K$  do
2   Estimate the conditional mean  $E(X_k|X_{k-1})$  and conditional variance
   Var( $X_k|X_{k-1}$ ) by  $\hat{m}(\hat{Z}_{k-1})$  and  $\hat{v}^2(\hat{Z}_{k-1})$ , respectively;
3   Draw a random sample  $\hat{X}_k$  from  $N\{\hat{m}(Z_{k-1}), \hat{v}^2(Z_{k-1})\}$ ;
4    $\hat{Z}_k \leftarrow (\hat{X}_k, t_k)^\top$ ;
5 end
```

incurring a lower rate of convergence.

4 Theoretical Results

We establish the existence and uniqueness of the solution to the proposed SDE as per (6) and the rate of consistency for the estimated sample path. The existence and uniqueness of the solution is built upon Gaussianity of the process X_t , i.e., for every finite set of time points t_1, \dots, t_k in \mathcal{T} , $(X_{t_1}, \dots, X_{t_k})^\top$ are jointly Gaussian distributed. The key step is to express the conditional mean $E(X_s|X_t)$ and conditional variance $\text{Var}(X_s|X_t)$ using the mean and covariance functions of X_t whence drift and diffusion coefficients in (6) are seen to satisfy the Lipschitz and linear growth conditions as per (2) and (3). Specifically,

$$E(X_s|X_t) = \mu(s) + \Sigma(s, t)\Sigma^{-1}(t, t)\{X_t - \mu(t)\}, \quad (10)$$

$$\text{Var}(X_s|X_t) = \Sigma(s, s) - \Sigma(s, t)\Sigma^{-1}(t, t)\Sigma(t, s). \quad (11)$$

If X_t is non-Gaussian, as long as a unique solution exists, the rate of convergence for the estimated sample path can be similarly derived by assuming Lipschitz continuity for the

conditional mean function $m(\cdot)$ and conditional variance function $v^2(\cdot)$; see Lemma 2.

To show that the drift and diffusion coefficients in (6) satisfy the Lipschitz and linear growth conditions as per (2) and (3), we require the following conditions.

(A1) The mean function $\mu(t) = E(X_t)$ is continuously differentiable on \mathcal{T} .

(A2) The covariance function $\Sigma(s, t) = \text{Cov}(X_s, X_t)$ is continuously differentiable in the lower triangular region $\{(s, t) : s \geq t, s, t \in \mathcal{T}\}$. Equivalently, the two partial derivative functions of $\Sigma(s, t)$

$$\Sigma'_s(s, t) = \frac{\partial \Sigma(s, t)}{\partial s}, \quad \Sigma'_t(s, t) = \frac{\partial \Sigma(s, t)}{\partial t}$$

exist and are continuous for every $s, t \in \mathcal{T}$ and $s \geq t$.

Conditions (A1) and (A2) are regularity conditions on the process X_t , where the latter implies that $\Sigma(s, t)$ is continuously differentiable in the upper triangular region $\{(s, t) : s \leq t, s, t \in \mathcal{T}\}$, as well but may not be differentiable across the diagonal $s = t$, which is for example a well-known property of Brownian motion. It is easy to verify that all examples of processes in subsection 2.2 satisfy Conditions (A1) and (A2); see Section S.1 of the Supplementary Material.

Theorem 1. *If the stochastic process X_t is Gaussian, satisfies Conditions (A1), (A2), and the initial value x_0 is a random variable independent of the σ -algebra \mathcal{F}_∞ generated by $\{B_s, s \geq 0\}$ with $E(x_0^2) < \infty$, then the stochastic differential equation (6) has a pathwise unique strong solution*

$$X_t = x_0 + \int_0^t \frac{\partial}{\partial r} E(X_r | X_s) \Big|_{r=s} ds + \int_0^t \left\{ \frac{\partial}{\partial r} \text{Var}(X_r | X_s) \Big|_{r=s} \right\}^{1/2} dB_s, \quad t \in \mathcal{T}$$

with the property that

$$X_t \text{ is adapted to the filtration } \mathcal{F}_t^{x_0} \text{ generated by } x_0 \text{ and } \{B_s, s \in [0, t]\} \quad (12)$$

and

$$\sup_{t \in \mathcal{T}} E(X_t^2) < \infty. \quad (13)$$

All proofs are given in Section S.3 of the Supplementary Material. The uniqueness of the solution is in the sense that if X_t and Y_t are two processes satisfying (6), (12), and (13) then

$$X_t = Y_t \quad \text{for all } t \in \mathcal{T} \quad \text{a.s.}$$

The solution X_t found above is a strong solution because the version B_t of Brownian motion is given in advance and the solution X_t constructed from it is $\mathcal{F}_t^{x_0}$ -adapted. The Gaussianity implies that X_t must be governed by a narrow-sense linear SDE (Kloeden and Platen 1999), where the drift coefficient $b(t, X_t) = a(t)X_t + c(t)$ and the diffusion coefficient is additive, i.e., $\sigma(t, X_t) = \sigma(t)$. Indeed, the drift and diffusion coefficients in (6) under Gaussian assumption are

$$\begin{aligned} b(t, X_t) &= \mu'(t) + \Sigma'_s(s, t)|_{s=t} \Sigma^{-1}(t, t) \{X_t - \mu(t)\}, \\ \sigma(t, X_t) &= \{\Sigma'(t, t) - 2\Sigma'_s(s, t)|_{s=t}\}^{1/2}, \end{aligned}$$

indicating the SDE (6) is narrow-sense linear. The general solution of a linear SDE can be found explicitly. Specifically, if X_t is Gaussian, as a solution of (6) it is of the form

$$X_t = \Phi(t) \left\{ x_0 + \int_0^t c(s) \Phi^{-1}(s) ds + \int_0^t \sigma(s) \Phi^{-1}(s) dB_s \right\}.$$

where $a(t) = \Sigma'_s(s, t)|_{s=t} \Sigma^{-1}(t, t)$, $c(t) = \mu'(t) - \Sigma'_s(s, t)|_{s=t} \Sigma^{-1}(t, t) \mu(t)$ and $\Phi(t) = e^{\int_0^t a(s) ds}$.

An important feature of the recursion in (7) is that it generates an exact simulation of X_t at t_1, \dots, t_K (Glasserman 2004) if X_t is a Gaussian process.

Lemma 1. *If the stochastic process X_t is Gaussian, then the recursion in (7) generates an exact simulation of the stochastic process X_t at t_1, \dots, t_K in the sense that the distribution of the X_1, \dots, X_K it produces is precisely that of the continuous-time process X_t at time points t_1, \dots, t_K .*

Lemma 1 ensures that we do not have to worry about the discretization error while deriving the rate of convergence for the estimated sample path if X_t is Gaussian. Regarding the asymptotic property of the estimated sample path as per (9), we investigate the rate of convergence for \hat{X}_K , which also applies to \hat{X}_k for any k . The proof relies on a recursive formula for the sequence $|\hat{X}_k - X_k|$, where the Lipschitz continuity of the conditional mean function $m(\cdot)$ and conditional variance function $v^2(\cdot)$ is utilized. To this end, we require the following conditions regarding the variance function $\Sigma(t, t)$ and the design of functional snippets.

- (B1) The variance function $\Sigma(t, t)$ is strictly positive on the half-open interval $(0, 1]$.
- (B2) The design for functional snippets is regular. Specifically, the observation time spacing $T_{i2} - T_{i1} = \delta$ is constant for all $i = 1, \dots, n$, where δ is the length of the spacing interval.

Condition (B1) is reasonable for real data applications, especially in our case where one is interested in modeling stochastic dynamics of the process X_t , and all example processes discussed in subsection 2.2 satisfy Condition (B1); see Section S.1 of the Supplementary Material. Under Gaussianity and Condition (B2), the conditional mean function $m(\cdot)$ and conditional variance function $v^2(\cdot)$ have the following explicit forms, writing $s = t + \delta$ and $X_t = x$ in (10), (11) and $z = (x, t)^\top$,

$$m(z) = \mu(t + \delta) + \Sigma(t + \delta, t)\Sigma^{-1}(t, t)\{x - \mu(t)\},$$

$$v^2(z) = \Sigma(t + \delta, t + \delta) - \Sigma(t + \delta, t)\Sigma^{-1}(t, t)\Sigma(t, t + \delta).$$

Lemma 2. *If the stochastic process X_t is Gaussian and satisfies (A1), (A2), and if (B1) and (B2) hold, then the conditional mean function $m(\cdot)$ is Lipschitz continuous in the variable x on $\mathbb{R} \times \{t_1, \dots, t_{K-1}\}$ with Lipschitz constant $L = \max_{t \in \{t_1, \dots, t_{K-1}\}} |\Sigma(t + \delta, t)\Sigma^{-1}(t, t)|$.*

Specifically, for all $z_1 = (x_1, t)^\top, z_2 = (x_2, t)^\top$ in $\mathbb{R} \times \{t_1, \dots, t_{K-1}\}$,

$$|m(z_1) - m(z_2)| \leq L|x_1 - x_2|.$$

Further, the conditional variance function $v^2(\cdot)$ satisfies

$$|v(z_1) - v(z_2)| = 0.$$

Lemma 2 guarantees that the sequence $|\hat{X}_k - X_k|$ does not grow too fast, whence one can bound $|\hat{X}_K - X_K|$ by recursion. Lemma 2 holds for all example processes discussed in subsection 2.2 with Lipschitz constant $L = 1$; see Section S.1 of the Supplementary Material for details.

To obtain the rate of convergence for the estimated sample path, one also needs to examine the asymptotic behavior of the conditional mean function estimate $\hat{m}(\cdot)$ and the conditional variance function estimate $\hat{v}^2(\cdot)$. Assume one has results for any fixed $z \in \mathbb{R} \times \mathcal{T}$ of the type

$$[E\{|\hat{m}(z) - m(z)|^2\}]^{1/2} = O(\alpha_n), \quad [E\{|\hat{v}^2(z) - v^2(z)|^2\}]^{1/2} = O(\beta_n). \quad (14)$$

If the residual-based estimator as described in Section S.2 of the Supplementary Material is adopted to estimate the conditional variance function $v^2(\cdot)$, it is well-known that the estimation of the conditional mean function $m(\cdot)$ has no influence on the estimation of $v^2(\cdot)$ (Fan and Yao 1998). Then $\beta_n = \alpha_n$ if the same regression method is performed to estimate $m(\cdot)$ and $v^2(\cdot)$. In the case of multiple linear regression, $\alpha_n = \beta_n = n^{-1/2}$, while $\alpha_n = \beta_n = n^{-1/3}$ for local linear regression.

Theorem 2. *If the stochastic process X_t is Gaussian and satisfies (A1), (A2), and if (B1), (B2) hold, then for the estimated sample path of the SDE (6) as defined in (9),*

$$\{E(|\hat{X}_K - X_K|^2)\}^{1/2} = O(\alpha_n + \beta_n),$$

where α_n and β_n are the rates of convergence for the conditional mean function estimate $\hat{m}(\cdot)$ and conditional variance function estimate $\hat{v}^2(\cdot)$ as per (14).

Theorem 2 implies that \hat{X}_K converges strongly to X_K , thereby establishing the pathwise convergence of the estimated sample path to the true process. We note that Condition (B2) is not strictly required, as the conditional mean and variance functions may be represented in terms of X_t , t , and s as per (10) and (11) and one can use $Z_i = (Y_{i1}, T_{i1}, T_{i2})$ as predictors in (8). It can be shown that the same Lipschitz continuity applies to $m(\cdot)$ and $v^2(\cdot)$ as in Lemma 2 and hence the same rate of convergence holds for \hat{X}_K .

Writing $\mathcal{L}(X_K)$, $\mathcal{L}(\hat{X}_K)$ for the distributions of X_K and of the corresponding estimator \hat{X}_K , respectively, we aim to quantify the discrepancy between $\mathcal{L}(\hat{X}_K)$ and $\mathcal{L}(X_K)$ as a measure of the performance of the estimator. The strong convergence results obtained in Theorem 2 can be used to obtain the rate of convergence of the 2-Wasserstein distance (Villani 2009) $d_W(\mathcal{L}(\hat{X}_K), \mathcal{L}(X_K))$, where the 2-Wasserstein distance between two probability measures ν_1, ν_2 on \mathbb{R} is $d_W^2(\nu_1, \nu_2) = \int_0^1 \{F_1^{-1}(p) - F_2^{-1}(p)\}^2 dp$, with F_1^{-1} and F_2^{-1} denoting the quantile functions of ν_1, ν_2 , respectively. If ν_1 and ν_2 are one-dimensional Gaussians with mean and covariance (m_1, σ_1^2) and (m_2, σ_2^2) then $d_W^2(\nu_1, \nu_2) = (m_1 - m_2)^2 + (\sigma_1 - \sigma_2)^2$. For the Wasserstein rate of convergence we obtain

Corollary 1. *Under the conditions of Theorem 2, the distribution of the estimated sample path as per (9) satisfies*

$$d_W\{\mathcal{L}(\hat{X}_K), \mathcal{L}(X_K)\} = O(\alpha_n + \beta_n),$$

where α_n and β_n are the rates of convergence for the conditional mean function estimate $\hat{m}(\cdot)$ and conditional variance function estimate $\hat{v}^2(\cdot)$ as per (14).

5 Finite Sample Performance

5.1 Simulation studies

We demonstrate the utility of the proposed approach in recovering underlying dynamics from functional snippets in a variety of simulation contexts. In our first example, we generate functional snippets from the Ho-Lee model and the Ornstein-Uhlenbeck process as discussed in subsection 2.2, respectively. To obtain functional snippets, we first simulate the sample path of $X_{t,i}$ at a regular time grid $\{t_k\}_{k=0}^K$ with $t_k = k\delta$ and $K\delta = 1$ for each $i = 1, \dots, n$. Denoting the simulated values for the n processes by $\{(X_{t_0,i}, X_{t_1,i}, \dots, X_{t_K,i})^\top\}_{i=1}^n$, functional snippets are generated as $\{(X_{T_i,i}, X_{T_i+\delta,i})^\top\}_{i=1}^n$ where for each i , T_i is a time point randomly selected from the time grid $\{t_k\}_{k=0}^{K-1}$. Since both the Ho-Lee model and the Ornstein-Uhlenbeck process are narrow-sense linear SDEs, exact methods for simulating their paths are available by examining their explicit solutions (Glasserman 2004). Specifically, for the Ho-Lee model $dX_t = g(t)dt + \sigma dB_t$, a simple recursive procedure for simulating values at $\{t_k\}_{k=0}^K$ is

$$X_{k+1} = X_k + \int_{t_k}^{t_{k+1}} g(s)ds + \sigma(t_k - t_{k+1})^{1/2}W_k, \quad (15)$$

where the $W_k \sim N(0, 1)$ are independent for all k and $X_0 = x_0$. Similarly for the Ornstein-Uhlenbeck process $dX_t = -\theta X_t dt + \sigma dB_t$, one can set

$$X_{k+1} = e^{-\theta(t_{k+1}-t_k)}X_k + \left\{ \frac{\sigma^2}{2\theta}(1 - e^{-2\theta(t_{k+1}-t_k)}) \right\}^{1/2} W_k. \quad (16)$$

The above procedures are exact in the sense that the joint distribution of the simulated values coincides with the joint distribution of the corresponding continuous-time process on the simulation grid. To investigate the effect of noise, we add independent errors to the generated functional snippets $\{(X_{T_i,i}, X_{T_i+\delta,i})^\top\}_{i=1}^n$. Specifically, we consider the contaminated functional snippets $\{(Y_{i1}, Y_{i2})^\top\}_{i=1}^n$ where $Y_{i1} = X_{T_i,i} + \varepsilon_{i1}$ and $Y_{i2} = X_{T_i+\delta,i} + \varepsilon_{i2}$ with $\varepsilon_{ij} \sim N(0, \nu^2)$ independently.

We examined the performance of the proposed approach across sample sizes $n = 100, 200, 500, 1000, 2000, 5000$ and noise levels $\nu = 0, 0.01, 0.1$. For each combination of sample size and noise level, the simulation was repeated $Q = 1000$ times. The time interval was chosen as $[0, 1]$ and the time spacing was $\delta = 0.05$. In each simulation, the recursive procedure as per (9) was performed $M = 5000$ times using the contaminated functional snippets $\{(Y_{i1}, Y_{i2})^\top\}_{i=1}^n$ with the initial condition $Z_0 = (0, 0)^\top$, from which $M = 5000$ estimated sample paths evaluated at the time grid $\{t_k\}_{k=1}^K$ were obtained. We write $\{(\hat{X}_{t_1, l}, \dots, \hat{X}_{t_K, l})^\top\}_{l=1}^M$ for the M sample path estimates. For each l , the corresponding true sample path $(X_{t_1, l}, \dots, X_{t_K, l})^\top$ was obtained using the recursive procedure in (15) or (16) with the same initial value and W_k . For the q th simulation of a particular sample size and noise level, the quality of the estimation was quantified by the root-mean-square error

$$\text{RMSE}_q = \left\{ \frac{1}{M} \sum_{l=1}^M (\hat{X}_{t_K, l} - X_{t_K, l})^2 \right\}^{1/2},$$

and the average quality of the estimation over the $Q = 1000$ simulations was assessed by the average root-mean-square error, $\text{ARMSE} = Q^{-1} \sum_{q=1}^Q \text{RMSE}_q$.

We chose $g(t) = \cos(t)$, $\theta = \sigma = 1$ and the initial condition $X_0 = 0$ for the Ho-Lee model and the Ornstein-Uhlenbeck process, respectively, and used multiple linear regression to estimate the conditional mean and conditional variance for both cases. The RMSE of $Q = 1000$ simulations and their averages (ARMSE) for different sample sizes and noise levels are summarized in Figure 1 and Table 1, respectively. We observe that the ARMSE decreases with increasing sample size, while the presence of noise does not impact the results much. To further illustrate the performance of the proposed dynamic modeling approach, we visualize the simulation results for the Ornstein-Uhlenbeck process with sample size $n = 100$ and noise level $\nu = 0.1$ in Figure 2, where $M = 100$ estimated sample paths are considered, along with the corresponding true sample paths. It is evident that the estimated sample paths recover the underlying stochastic dynamics from very sparse data,

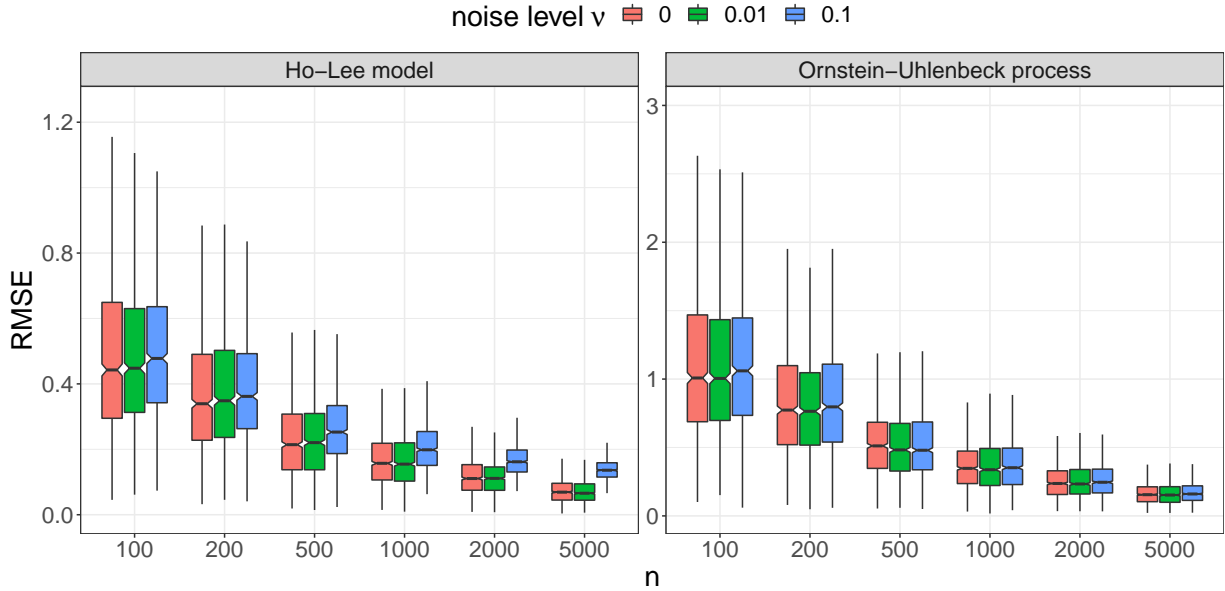


Figure 1: Boxplots of ARMSE for different sample sizes and noise levels.

Table 1: Average root-mean-square error (ARMSE) for different sample sizes and noise levels.

Sample size	Noise level	Ho-Lee model			O-U process		
		0	0.01	0.1	0	0.01	0.1
100		0.56	0.56	0.58	1.28	1.31	1.33
200		0.39	0.40	0.41	0.89	0.89	0.91
500		0.24	0.23	0.27	0.56	0.53	0.54
1000		0.17	0.17	0.21	0.37	0.37	0.38
2000		0.12	0.12	0.17	0.25	0.26	0.26
5000		0.07	0.07	0.14	0.16	0.16	0.17

demonstrating that the proposed approach performs well.

5.2 Simulating snippets from the Berkeley growth study data

We also illustrate the proposed modeling approach by drawing snippet samples from the Berkeley growth study data (Tuddenham and Snyder 1954), where growth curves quantified by height in cm of 93 children (54 females and 39 males) are measured quarterly from 1 to 2 years, annually from 2 to 8 years and biannually from 8 to 18 years. We applied the proposed method to females and males separately since female and male growth trends differ

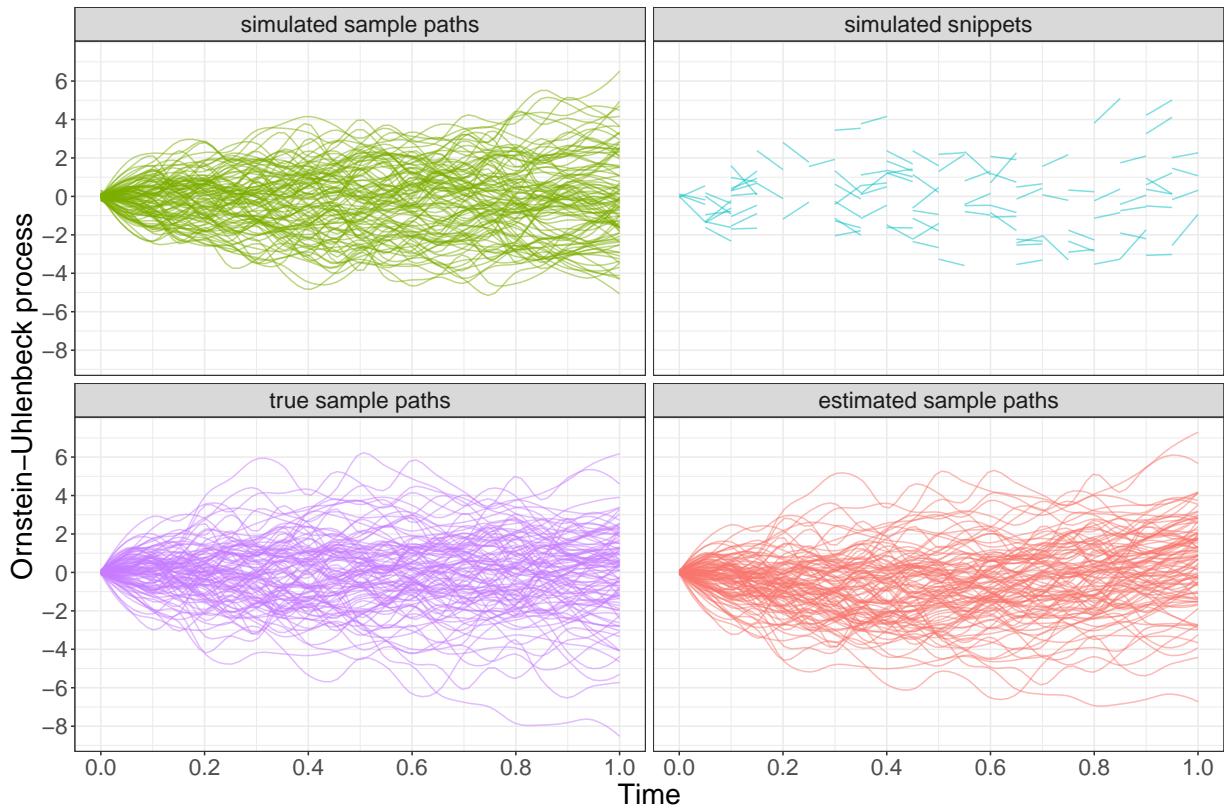


Figure 2: $M = 100$ simulated sample paths (top left), simulated snippets (top right), true sample paths (bottom left), and estimated sample paths (bottom right) for the Ornstein-Uhlenbeck process. The sample size is $n = 100$ and the noise level is $\nu = 0.1$.

significantly, with females reaching puberty far sooner than males. To visually evaluate the quality of the estimated sample paths, we enlarge the sample size by generating synthetic growth curves for females and males, respectively. Specifically, the mean function, the first three eigenfunctions, and functional principal component scores for each female are first estimated from the original growth data for females, where the first three components account for 97.5% of the variation. We then resample the functional principal component scores from their joint distribution and use the resampled scores to construct an augmented sample of 300 growth curves for females and analogously for males. Artificial snippets are created by randomly selecting two measurements, one year apart, for each synthetic growth curve.

To recover the underlying growth dynamics from snippet samples, we carried out the

proposed recursive procedure in (9) 1000 times to obtain 1000 estimated growth curves, where local linear regression is utilized to estimate the conditional mean and conditional variance. The starting time is $t_0 = 1$ year old for both females and males, while the time spacing is the measurement spacing in the artificial snippets, i.e., $\Delta = 1$ year. To reconstruct the unconditional dynamic distributions for the Berkeley growth study data, a starting height X_0 was randomly chosen at the age of one year. The bandwidth for both the conditional mean and conditional variance estimation was chosen as $h = (20, 0.5)^T$ using leave-one-out cross-validation. Figure 3, from left to right, shows the synthetic growth curves, artificial growth snippets, and estimated growth curves for females and males, respectively. We observe that the estimated growth curves fully recover the underlying growth dynamics from the artificial growth snippets, and the recovered estimates match those for the synthetic growth curves, demonstrating the utility of the proposed method.

6 Data Applications

6.1 Nepal growth study data

Screening children’s development status and monitoring height growth is essential for pediatric public health (Chen and Müller 2012) and due to limited resources often must be based on incomplete data. We demonstrate the potential of the proposed dynamic modeling approach to characterize underlying growth patterns and reveal specific growth trends with snippet data from a Nepal growth study (West Jr et al. 1997). This data set contains height measurements for 2258 children from rural Nepal taken at five adjacent times points from birth to 76 months, spaced approximately four months apart. To facilitate the exploration of these data, we use the first 1000 records, containing measurements for 107 males and 93 females. Due to missing data, the actual number of measurements per child ranges between 1 and 5. The children with at least two measurements in a row are included in the

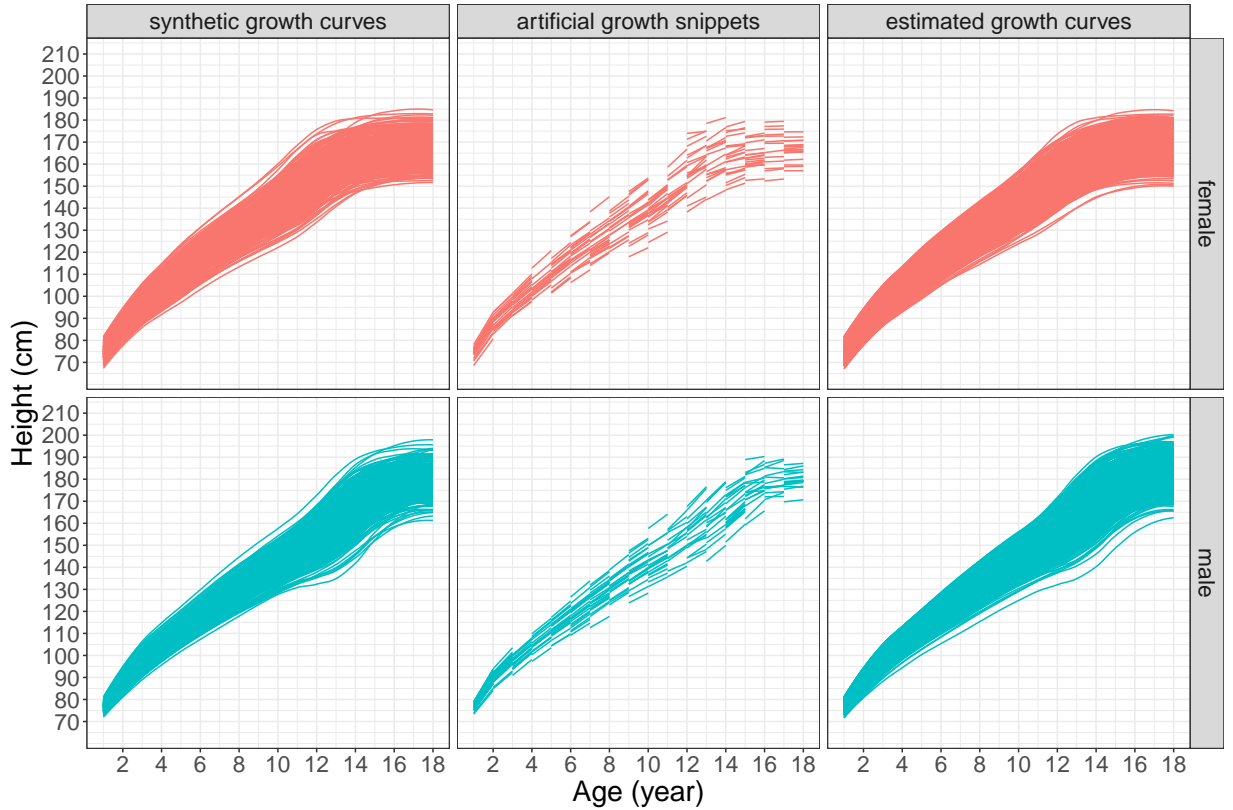


Figure 3: Synthetic growth curves (left), artificial growth snippets (middle), and estimated growth curves (right) for the Berkeley growth study data.

model, while the rest are used for model validation. Again we analyze the data for females and males separately due to the sexual dimorphism of growth.

Up to this point we assumed that each subject is only observed twice for ease of presentation. For denser scenarios where the number of measurements per subject $N_i > 2$, one option is to divide the N_i measurements into $N_i - 1$ pairs of contiguous measurements for each i and combine these pairs into a new sample for conditional mean and conditional variance estimation. This is a useful approach if the sample size n is relatively small, which is often the case in practice. We employ this strategy to make full use of the Nepal growth study data as well as the spinal bone mineral density data that we will explore in the next subsection.

While in subsection 5.2 we demonstrated the efficacy of the proposed dynamic modeling approach to recover the underlying growth dynamics from snippet data using Berkeley

growth study data, we highlight here another important application of the proposed approach – growth monitoring. Given a child’s initial development status, the proposed approach predicts child-specific growth patterns far into the future. As a child grows older and fresh measurements become available, we are able to screen the child’s development by comparing newly available measurements with the predicted growth. We demonstrate this with a randomly selected female and male who have no contiguous measurements and hence are not included in the model fitting. Specifically, the selected female was measured only once at 4 months, while the male was measured at 12 and 20 months.

To obtain future growth patterns for these two children, the recursive procedure in (9) was implemented 100 times using the growth snippets with at least two measurements in a row to obtain 100 estimated growth curves, where local linear regression was adopted to estimate the conditional mean and conditional variance. The starting time is $t_0 = 4$ months old for the selected female and $t_0 = 12$ months old for the selected male, where the time spacing was set at $\Delta = 4$ months, corresponding to the intended measurement spacing of the Nepal growth study. The starting height X_0 is chosen as the initial height measurement, i.e., 52.9 cm and 63 cm for the selected female and male, respectively. The bandwidth for both the conditional mean and conditional variance estimation is chosen using leave-one-out cross-validation.

The estimated growth curves and the corresponding 5%, 50%, 95% percentile curves (dashed), along with the observed growth snippets are shown in Figure 4. Although the available information is very limited due to the sparse and snippet nature of the data, the proposed approach is capable of capturing relevant dynamics from the observed growth snippets and revealing future growth trends of the selected female and male. For the selected male, one fresh height measurement is available at later age (20 months old). In comparison to the estimated growth patterns, the newly available height measurement (65.1 cm) falls below 5% percentile curve, indicating that this child may be developmentally

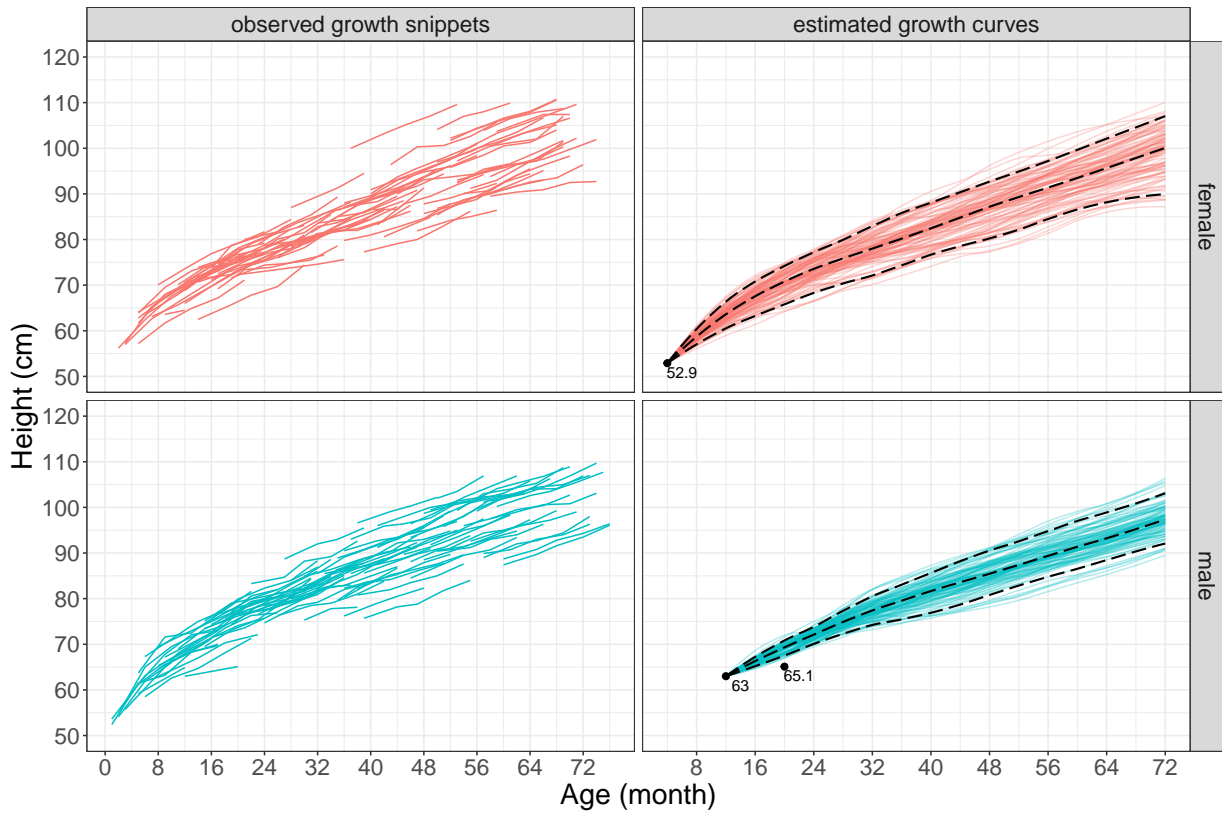


Figure 4: Observed growth snippets (left) and estimated growth curves (right) for the Nepal growth study data. The black dashed curves indicate 5%, 50% and 95% percentiles. Height measurements for the selected female and male are also highlighted.

delayed and require further follow-up.

6.2 Spinal bone mineral density data

We also implemented the proposed technique to analyze the longitudinal data set gathered and documented in Bachrach et al. (1999), where spinal bone mineral density was measured annually in four years for 423 healthy individuals. Since the visit schedules were not strictly followed, the number of measurements per individual varies from 1 to 4 and the time spacing between some measurements deviate substantially from one year, so that this is an accelerated study with irregular snippets. We included 153 females and 127 males with ages ranging from 8.8 to 26.2 years old who completed at least 2 measurements in the modeling, while the remaining subjects with only one measurement were used for model

validation.

To infer individual-specific stochastic dynamics of spinal bone mineral density from the irregularly observed density snippets, we again randomly selected one female and male who were measured at ages 10 and 9 years, respectively. Similarly, the recursive procedure in (9) was run 100 times to obtain 100 estimated bone density curves. Local linear regression was used to obtain conditional mean and variance, with cross-validation bandwidth selection. The starting time was chosen as $t_0 = 10$ years old for the selected female and $t_0 = 9$ years old for the selected male, with an end time of $t_K = 24$ years, with one-year time increment, corresponding to the scheduled measurement spacing of the data. The starting values of bone mineral density are 0.778 and 0.642 for the selected female and male, respectively, corresponding to their initial density measurements.

Figure 5 depicts the observed snippets and estimated bone density curves, along with 5%, 50%, 95% percentile curves (dashed). We find that the proposed dynamic modeling approach accommodates the irregularity inherent in these data; see the right panel of Figure 5. Comparing the recovered bone density curves for the selected female and male, we find that for the female these curves reach a plateau at around 16 years, while for the male they level off at around 18 years. This finding is in agreement with the literature (Bachrach et al. 1999).

7 Discussion

In this article, we propose a flexible and robust approach to recover the dynamic distribution from functional snippets using stochastic differential equations when the underlying processes are Gaussian. The proposed framework circumvents the issue of estimating covariance surfaces in the presence of missing data in the off-diagonal regions, resulting in a consistent reconstruction of sample paths from observed snippets. Furthermore, both

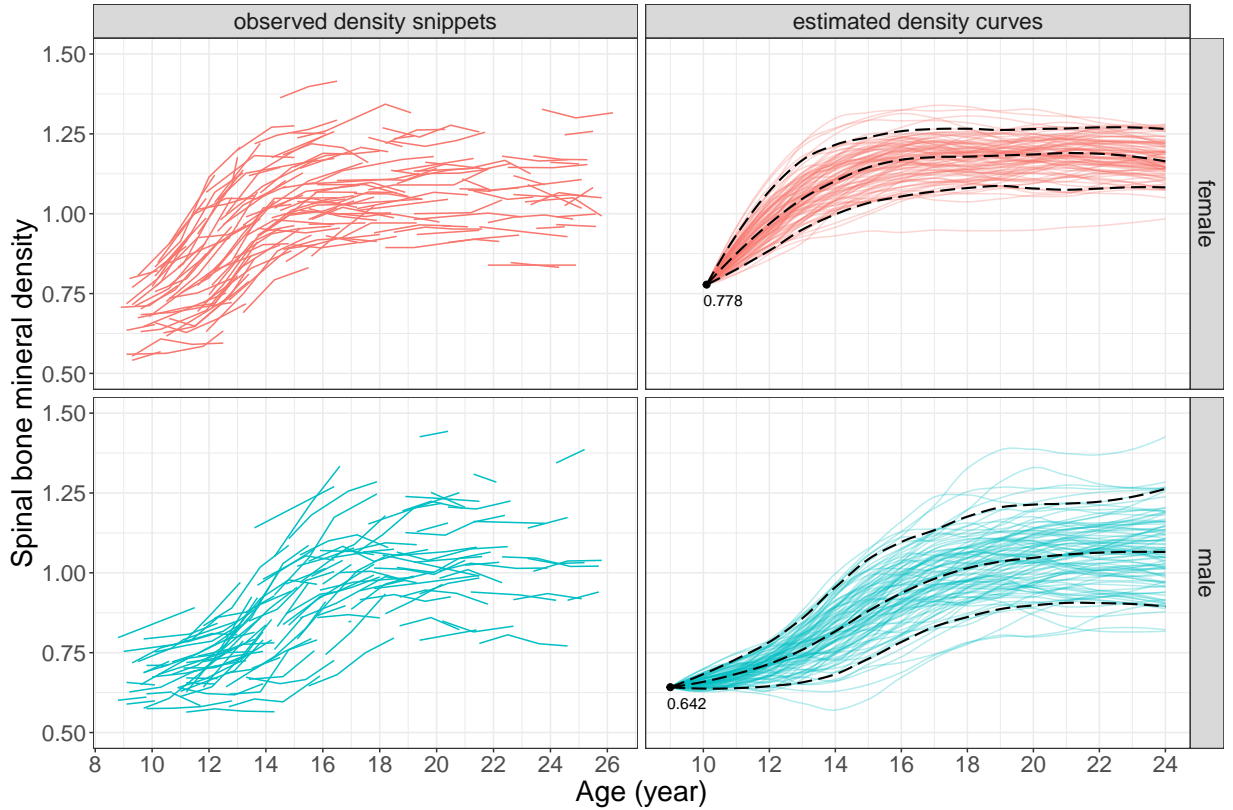


Figure 5: Observed growth snippets (left) and estimated bone density curves (right) for the Nepal growth study data. The black dashed curves indicate 5%, 50% and 95% percentiles. The bone density measurements of the selected female and male are also highlighted.

theoretical analysis and numerical simulations support and substantiate the effectiveness and usefulness of the proposed SDE approach for the analysis of functional snippets.

In the theoretical analysis, we have not considered noise in the observed snippets, which could be present in practice and hence introduce an errors-in-variables problem (Griliches and Hausman 1986). Future studies would focus on the theoretical characteristics of the proposed estimators with noise contamination. Although the methodology to model functional snippets using stochastic differential equations is the emphasis of this paper, we investigate the effect of noise in the observed snippets in simulation studies and find that the proposed approach is robust to the contamination of noises.

Under Gaussian assumption, the conditional mean and conditional variance of X_t are functions of its mean and covariance. Therefore, substituting the relevant estimates of mean

and covariance would be one possible way to estimate the conditional mean and conditional variance. Nevertheless, we discover from simulations that the proposed regression approach performs significantly better than such a plug-in strategy. One plausible cause is the lack of sufficient data in the case of functional snippets to accurately estimate the mean and covariance.

References

- Abramson, I. and Müller, H.-G. (1994). Estimating direction fields in autonomous equation models, with an application to system identification from cross-sectional data. *Biometrika*, 81(4):663–672.
- Bachrach, L. K., Hastie, T., Wang, M.-C., Narasimhan, B., and Marcus, R. (1999). Bone mineral acquisition in healthy Asian, Hispanic, Black, and Caucasian youth: a longitudinal study. *Journal of Clinical Endocrinology & Metabolism*, 84(12):4702–4712.
- Castro, P. E., Lawton, W. H., and Sylvestre, E. A. (1986). Principal modes of variation for processes with continuous sample curves. *Technometrics*, 28:329–337.
- Chen, K. and Lei, J. (2015). Localized functional principal component analysis. *Journal of the American Statistical Association*, 110(511):1266–1275.
- Chen, K. and Müller, H.-G. (2012). Conditional quantile analysis when covariates are functions, with application to growth data. *Journal of the Royal Statistical Society: Series B*, 74:67–89.
- Comte, F. and Genon-Catalot, V. (2020). Nonparametric drift estimation for i.i.d. paths of stochastic differential equations. *Annals of Statistics*, 48(6):3336–3365.
- Dawson, M. and Müller, H.-G. (2018). Dynamic modeling of conditional quantile trajectories, with application to longitudinal snippet data. *Journal of the American Statistical Association*, 113(524):1612–1624.
- Denis, C., Dion-Blanc, C., and Martinez, M. (2021). A ridge estimator of the drift from discrete repeated observations of the solution of a stochastic differential equation. *Bernoulli*, 27(4):2675–2713.
- Descary, M.-H. and Panaretos, V. M. (2019). Recovering covariance from functional fragments. *Biometrika*, 106(1):145–160.
- Fan, J. and Gijbels, I. (1996). *Local Polynomial Modelling and its Applications*. Chapman & Hall, London.
- Fan, J. and Yao, Q. (1998). Efficient Estimation of Conditional Variance Functions in Stochastic Regression. *Biometrika*, 85(3):645–660.

- Galbraith, S., Bowden, J., and Mander, A. (2017). Accelerated longitudinal designs: An overview of modelling, power, costs and handling missing data. *Statistical Methods in Medical Research*, 26(1):374–398.
- Glasserman, P. (2004). *Monte Carlo Methods in Financial Engineering*, volume 53. Springer.
- Griliches, Z. and Hausman, J. A. (1986). Errors in variables in panel data. *Journal of Econometrics*, 31(1):93–118.
- Hall, P. and Horowitz, J. L. (2007). Methodology and convergence rates for functional linear regression. *Annals of Statistics*, 35(1):70–91.
- Hall, P. and Hosseini-Nasab, M. (2006). On properties of functional principal components analysis. *Journal of the Royal Statistical Society: Series B*, 68(1):109–126.
- Hall, P., Müller, H.-G., and Wang, J.-L. (2006). Properties of principal component methods for functional and longitudinal data analysis. *Annals of Statistics*, 34:1493–1517.
- He, G., Müller, H.-G., and Wang, J.-L. (2000). Extending correlation and regression from multivariate to functional data. In Puri, M. L., editor, *Asymptotics in Statistics and Probability*, pages 301–315. VSP International Science Publishers.
- Ho, T. S. and Lee, S.-B. (1986). Term structure movements and pricing interest rate contingent claims. *Journal of Finance*, 41(5):1011–1029.
- Hsing, T. and Eubank, R. (2015). *Theoretical foundations of functional data analysis, with an introduction to linear operators*, volume 997. John Wiley & Sons.
- Kleffe, J. (1973). Principal components of random variables with values in a separable Hilbert space. *Mathematische Operationsforschung und Statistik*, 4:391–406.
- Kloeden, P. E. and Platen, E. (1999). *Numerical Solution of Stochastic Differential Equations*. Springer-Verlag.
- Kneip, A., Liebl, D., et al. (2020). On the optimal reconstruction of partially observed functional data. *Annals of Statistics*, 48(3):1692–1717.
- Li, Y. and Hsing, T. (2010). Uniform convergence rates for nonparametric regression and principal component analysis in functional/longitudinal data. *Annals of Statistics*, 38(6):3321–3351.
- Liebl, D. and Rameseder, S. (2019). Partially observed functional data: The case of systematically missing parts. *Computational Statistics & Data Analysis*, 131:104–115.
- Lin, Z., Wang, J.-L., and Zhong, Q. (2021). Basis expansions for functional snippets. *Biometrika*, 108(3):709–726.
- Müller, H.-G. (1987). Weighted local regression and kernel methods for nonparametric curve fitting. *Journal of the American Statistical Association*, 82(397):231–238.

- Müller, H.-G. and Yao, F. (2010). Empirical dynamics for longitudinal data. *Annals of Statistics*, 38:3458–3486.
- Oksendal, B. (2013). *Stochastic Differential Equations: An Introduction with Applications*. Springer Science & Business Media.
- Panik, M. J. (2017). *Stochastic Differential Equations: An Introduction with Applications in Population Dynamics Modeling*. John Wiley & Sons.
- Pavliotis, G. A. (2014). *Stochastic Processes and Applications: Diffusion Processes, the Fokker-Planck and Langevin Equations*, volume 60. Springer.
- Ramsay, J. O. and Silverman, B. W. (2005). *Functional Data Analysis*, volume 426 of *Springer Series in Statistics*. Springer, New York, second edition.
- Tuddenham, R. and Snyder, M. (1954). Physical growth of California boys and girls from birth to age 18. *University of California Publications in Child Development*, 1:183–364.
- Uhlenbeck, G. E. and Ornstein, L. S. (1930). On the theory of the Brownian motion. *Physical Review*, 36(5):823.
- Verzelen, N., Tao, W., and Müller, H.-G. (2012). Inferring stochastic dynamics from functional data. *Biometrika*, 99(3):533–550.
- Villani, C. (2009). *Optimal Transport: Old and New*, volume 338. Springer.
- Vittinghoff, E., Malani, H. M., and Jewell, N. P. (1994). Estimating patterns of CD4 lymphocyte decline using data from a prevalent cohort of HIV infected individuals. *Statistics in Medicine*, 13(11):1101–1118.
- Wang, J.-L., Chiou, J.-M., and Müller, H.-G. (2016). Functional Data Analysis. *Annual Review of Statistics and its Application*, 3:257–295.
- West Jr, K. P., LeClerq, S. C., Shrestha, S. R., Wu, L. S.-F., Pradhan, E. K., Khatry, S. K., Katz, J., Adhikari, R., and Sommer, A. (1997). Effects of vitamin A on growth of vitamin A-deficient children: field studies in Nepal. *Journal of Nutrition*, 127(10):1957–1965.
- Yao, F., Müller, H.-G., and Wang, J.-L. (2005a). Functional data analysis for sparse longitudinal data. *Journal of the American Statistical Association*, 100(470):577–590.
- Yao, F., Müller, H.-G., and Wang, J.-L. (2005b). Functional linear regression analysis for longitudinal data. *Annals of Statistics*, 33(6):2873–2903.
- Zhang, X. and Wang, J.-L. (2016). From sparse to dense functional data and beyond. *Annals of Statistics*, 44(5):2281–2321.
- Zhou, H., Wei, D., and Yao, F. (2022). Theory of functional principal components analysis for discretely observed data. *arXiv preprint arXiv:2209.08768*.